Bound Analysis for Anchor Selection in Cooperative Localization

Ping Zhang, Along Cao, and Tao Liu(✉)

School of Computer Science, Anhui Polytechnic University, Wuhu, China
{pingzhang,liutao}@ahpu.edu.cn, 154351635@qq.com

Abstract. Anchor selection refers to choosing a small portion of the nodes with known locations to ensure the unique localizability and/or improve the accuracy of cooperative localization. Focusing on the localization accuracy, conventional practice suggests that the anchors should be deployed on the perimeter of the network. This paper derives the perimeter anchor deployment strategy by performing a bound analysis for the Cramér-Rao lower bound (CRLB) which quantifies the localization accuracy. It is proved that the uniform perimeter anchor deployment strategy is the optimal to fix an isotropically discriminable relative configuration whose nodes are randomly deployed onto a two-dimensional plane. For the relative configuration specified by the internode distance measurements, we introduce an error metric to evaluate the anchor selection performance, together with an upper bound that is independent of anchor selection.

Keywords: Wireless sensor networks · Relative configuration · Kullback-Cleibler distance · Singular value decomposition · Internode distances

1 Introduction

Cooperative localization has attracted great interest recently because it meets the requirement of obtaining the node locations for the emerging wireless sensor networks and other large scale networks to perform various monitoring/surveillance tasks [1]. It uses the internode measurements, *e.g.*, connectivity, received signal strength (RSS), angel-of-arrival (AOA), angel-difference-of-arrival (ADOA), time-of-arrival (TOA), or time-difference-of-arrival (TDOA), to expand the localization area and/or improve the localization accuracy [2,3]. But the internode measurements provide only the relative location information [2,4]. To get the absolute locations, one should assign absolute locations to a small portion of the nodes, called anchors, *a priori*. Anchor selection, or named anchor deployment/placement, refers to determining which nodes should be specified as the anchors to ensure the coverage and/or improve the accuracy of cooperative localization.

F. Chen and Y. Luo (Eds.): Industrial IoT 2017, LNICST 202, pp. 1–10, 2017.
DOI: 10.1007/978-3-319-60753-5_1

Ensuring the coverage of cooperative localization is usually known as the unique localizability problem. Given the observed data, *i.e.*, the internode measurements and the anchor locations, the network is said to be uniquely localizable if there is a unique set of node locations consistent with the given data. This problem is closely related to the graph rigidity [5]. That is, a network is unique localizable if and only if the corresponding graph (whose edges are composed of the ones related to the internode measurements and the ones between at least three, in two dimensional case, noncollinear anchors) is globally rigid. Testing the unique localizability of a network requires only polynomial time, but the realization problem is NP-hard [6]. To cope with this realization problem, a triangulation-based graph is constructed, where the realization time is polynomial with respect to the node number [6]. An extension of the triangulation-based graph is involving the wheel structure [7], and some special graphs can even be realized in linear time [8]. The minimum number of the anchors to guarantee the unique localizability was investigated in [9], and which nodes can be uniquely located under given anchor locations was explored in [10].

Besides the coverage, the localization accuracy is another object that can be improved by anchor selection. Focusing on the localization accuracy, most existing work suggested that the anchors should be placed on the perimeter of the network. By using the multi-hop distance approximation, the outmost corner anchor placement can be derived after transforming cooperative localization into conventional localization [11]. Simulations in [12] demonstrated that anchors deployed in the network center or covering a small area may cause large error. Instead of the outmost corner anchor placement, the near perimeter, but not the outmost, placement exhibited the best performance in the simulations. For some specific algorithms in cooperative localization [2,13], the experiments also support the perimeter anchor deployment strategy.

From another point of view, the internode measurements specify the network relative configuration [4], which depicts the "shape" of the network without considering the network's location and orientation [3]. This leads to a relative/transformation subspace decomposition, where the anchor selection seems mainly affect the error in the transformation subspace but not the error in the relative subspace [4,14]. Based on this discovery, a perimeter anchor deployment can be derived by minimizing the principal angle between anchor constraint subspace and the transformation subspace [15]. Besides, if we introduce the anchor location uncertainty but ignore the internode measurement noise, the uniform perimeter anchor deployment strategy can be proved to be the optimal when the nodes are randomly deployed on a two-dimensional plane [16].

This paper derives a uniform perimeter anchor deployment strategy by minimizing an approximation of the Cramér-Rao lower bound (CRLB) which quantifies the localization error. This approximation is obtained from a bound analysis for the CRLB, and is actually the CRLB under the assumption that the corresponding relative configuration is isotropically discriminable. Considering that the relative configuration specified by the noisy internode distance measurements is not isotropically discriminable in general, we introduce an error metric to evaluation the approximation performance, together with an upper bound that is independent of anchor selection.

The remainder of this paper is organized as follows. Section 2 derives the CRLB for the node locations under a statistical model for cooperative localization. For the derived CRLB, Sect. 3 introduces an approximation, based on which a uniform perimeter anchor deployment strategy can be derived when the nodes are randomly deployed on a two-dimensional plane. In Sect. 4, we conclude this paper.

2 Background

This section details the statistical model of the internode distance measurements and derives the CRLB for the unknown node locations under given anchor locations.

Let us consider a network composed of n nodes, whose relative configuration is specified by the internode distance measurements modeled as

$$y_{i,j} = d_{i,j} + \epsilon_{i,j}, \quad (i,j) \in \mathcal{E} \tag{1}$$

where $d_{i,j} = \|\mathbf{s}_i - \mathbf{s}_j\|$ denotes the Euclidean distance between the ith and the jth node, $\epsilon_{i,j}$, $(i,j) \in \mathcal{E}$, are independent and identical distributed Gaussian stochastic noises with zero mean and variance σ^2, and $\mathcal{E}$ denotes the index set of connected edges corresponding to the distance measurements. In this section, we assume the distance measurements are sufficient to guarantee the global rigidity of the network, and the distance measurements are symmetrical so that any index pair $(i,j) \in \mathcal{E}$ fulfills $i < j$.

The logarithm of the probability density function specified by (1) is

$$\log p(\mathbf{y}; \mathbf{s}) = -\frac{1}{2\sigma^2} \sum_{(i,j)\in\mathcal{E}} (y_{i,j} - d_{i,j})^2 + c \tag{2}$$

where the measurement vector $\mathbf{y} = [y_{i,j}]_{(i,j)\in\mathcal{E}}$, and the constant c is independent of $\mathbf{s}$. After taking the negative expectation of the second derivation of (2), we get the FIM of $\mathbf{s}$

$$\mathbf{J_s} = -\mathrm{E}\left[\frac{\partial^2 \log p(\mathbf{y}; \mathbf{s})}{\partial \mathbf{s} \partial \mathbf{s}^T}\right] = \sigma^{-2}\mathbf{F}^T\mathbf{F} \tag{3}$$

where the rows of $\mathbf{F}$ are the partial derivatives of $d_{i,j}$, $(i,j) \in \mathcal{E}$, with respect to the location vector $\mathbf{s}$, given by

$$\frac{\partial d_{i,j}}{\partial \mathbf{s}^T} = \left[\mathbf{0}_{1\times 2(i-1)}, \boldsymbol{\tau}_{i,j}^T, \mathbf{0}_{1\times 2(j-i-1)}, \boldsymbol{\tau}_{j,i}^T, \mathbf{0}_{1\times 2(n-j)}\right] \tag{4}$$

where $\boldsymbol{\tau}_{i,j} = -\boldsymbol{\tau}_{j,i} = \frac{\mathbf{s}_i - \mathbf{s}_j}{\|\mathbf{s}_i - \mathbf{s}_j\|}$.

Internode distances specify only the relative configuration of the network, leaving the network location and orientation unknown. According to this fact, there exists a relative-transformation decomposition of the location subspace

$\mathbb{R}^{2n}$ [3,4]. The transformation subspace relates to the translation and rotation of the network, which is spanned by the columns of $\mathbf{V} = [\mathbf{1}_x, \mathbf{1}_y, \mathbf{v}]$ where $\mathbf{1}_x = [1, 0, \ldots, 1, 0]^T \in \mathbb{R}^{2n}$, $\mathbf{1}_y = [0, 1, \ldots, 0, 1]^T \in \mathbb{R}^{2n}$, and $\mathbf{v} = [s_{1,y}, -s_{1,x}, \ldots, s_{n,y}, -s_{n,x}]^T \in \mathbb{R}^{2n}$. The relative subspace relates to shape (including size) of the network, which is spanned by the columns of $\mathbf{U}$ which form an orthonormal basis of the null space of $\mathbf{V}^T$. Using a suitable $\mathbf{U}$, we can perform a compact singular value decomposition (SVD) of the FIM $\mathbf{J_s}$ in the relative subspace as

$$\mathbf{J_s} = \mathbf{U}\boldsymbol{\Lambda}\mathbf{U}^T \tag{5}$$

where $\boldsymbol{\Lambda}$ is a diagonal matrix with diagonal elements $\lambda_1 \geq \lambda_2 \geq \cdots \geq \lambda_{2n-3} > 0$.

The unknown node locations can be uniquely estimated after setting at least three nodes as anchors. Here, we use $\mathcal{U}$ and $\mathcal{A}$ denote the index set of the unknown nodes and the anchor nodes, respectively, where $\mathcal{U} \bigcup \mathcal{A} = \{1, 2, \cdots, n\}$. After given m anchors, the CRLB of the unknown node locations can be represented as

$$\mathbf{C} = (\mathbf{H}^T\mathbf{J_s}\mathbf{H})^{-1} \tag{6}$$

where $\mathbf{H}$ is a $2n$-by-$2(n-m)$ matrix which is stacked in column by

$$\left[\mathbf{0}_{2\times 2(j-1)}, \mathbf{I}_2, \mathbf{0}_{2\times 2(n-j)}\right]^T, j \in \mathcal{U}$$

in column.

Throughout this paper, the optimal anchor set refers to the one minimizing the CRLB trace $\mathrm{tr}(\mathbf{C})$, which lower bounds the variance of any unbiased estimate and can be asymptotically achieved by maximum likelihood estimation (MLE).

3 Bound Analysis

It is somewhat difficult to derive the perimeter anchor deployment strategy from the analytic expression of (6). To cope with this problem, we introduce an approximation $b(\mathcal{A})$ of $\mathrm{tr}(\mathbf{C})$, where the difference between $\mathrm{tr}(\mathbf{C})$ and $b(\mathcal{A})$ is bounded as below.

Proposition 1. *The ratio between* $\mathrm{tr}(\mathbf{C})$ *and* $b(\mathcal{A})$ *is bounded as*

$$\lambda_1^{-1} \leq \frac{\mathrm{tr}\,(\mathbf{C})}{b(\mathcal{A})} \leq \lambda_{2n-3}^{-1}. \tag{7}$$

where λ_1 *and* λ_{2n-3} *are the first and the* $(2n-3)$*th largest eigenvalues of the distance FIM* $\mathbf{J_s}$*, and*

$$b(\mathcal{A}) = \mathrm{tr}\left(\left(\mathbf{H}^T\mathbf{U}\mathbf{U}^T\mathbf{H}\right)^{-1}\right)$$
$$\frac{n}{m}\left(\frac{(\bar{s}_{\mathcal{A},x} - \bar{s}_x)^2 + (\bar{s}_{\mathcal{A},y} - \bar{s}_y)^2 + \rho^2}{\rho_{\mathcal{A}}^2} + 2\right) + 2(n-m) - 3 \tag{8}$$

where $\bar{s}_x = \frac{1}{n}\sum_{i=1}^n s_{i,x}$, $\bar{s}_y = \frac{1}{n}\sum_{i=1}^n s_{i,y}$, $\bar{s}_{\mathcal{A},x} = \frac{1}{m}\sum_{j\in\mathcal{A}} s_{j,x}$, $\bar{s}_{\mathcal{A},y} = \frac{1}{m}\sum_{j\in\mathcal{A}} s_{j,y}$, $\rho^2 = \frac{1}{n}\sum_{i=1}^n (s_{i,x} - \bar{s}_x)^2 + (s_{i,y} - \bar{s}_y)^2$, *and* $\rho_{\mathcal{A}}^2 = \frac{1}{m}\sum_{j\in\mathcal{A}} (s_{j,x} - \bar{s}_{\mathcal{A},x})^2 + (s_{j,y} - \bar{s}_{\mathcal{A},y})^2$.

The derivation of (7) and (8) can be found in Appendix A.

Minimizing $b(\mathcal{A})$ leads to the uniform perimeter anchor deployment strategy. In (8), $b(\mathcal{A})$ can be viewed as a function of $(\bar{s}_{\mathcal{A},x}-\bar{s}_x)^2+(\bar{s}_{\mathcal{A},y}-\bar{s}_y)^2$ and $\rho_{\mathcal{A}}$ that are affected by the anchor selection. To minimize $b(\mathcal{A})$, $(\bar{s}_{\mathcal{A},x}-\bar{s}_x)^2+(\bar{s}_{\mathcal{A},y}-\bar{s}_y)^2$ should be minimized, and $\rho_{\mathcal{A}}$ should be maximized. $(\bar{s}_{\mathcal{A},x}-\bar{s}_x)^2+(\bar{s}_{\mathcal{A},y}-\bar{s}_y)^2$ evaluates the squared distance between the centroids of the anchors and the nodes. It can be reduced to zero if $\bar{s}_{\mathcal{A},x}=\bar{s}_x$ and $\bar{s}_{\mathcal{A},y}=\bar{s}_y$. $\rho_{\mathcal{A}}$ quantifies the diameter of the network composed of the anchors. To maximize it, the anchors should be deployed on the perimeter of the network. When the nodes are randomly deployed in a two-dimensional plane, deploying the anchors uniformly around the perimeter of the network meets the requirements above, so that it can be viewed as an optimal strategy to reduce $b(\mathcal{A})$.

What is the difference between minimizing $b(\mathcal{A})$ and minimizing $\mathrm{tr}(\mathbf{C})$? Here we provide four examples to demonstrate the difference between $b(\mathcal{A})$ and $\mathrm{tr}(\mathbf{C})$, seen in Fig. 1. These four examples differ in the node configuration, where the nodes are deployed regularly in a circular region in Fig. 1a, randomly in a circular region in Fig. 1b, regularly in a square region in Fig. 1c, and randomly in a square region in Fig. 1d. Figure 1e, f, g, and h display the CRLB trace $\mathrm{tr}(\mathbf{C})$, its lower bound $\lambda_1^{-1}b(\mathcal{A})$, and upper bound $\lambda_{2n-3}^{-1}b(\mathcal{A})$ as the functions of all anchor triplets selected from the nodes, sorted by the descending order of $b(\mathcal{A})$. From these figures, it can be found that there is a similar tendency in the variation of $\mathrm{tr}(\mathbf{C})$ and $b(\mathcal{A})$, so that minimizing $\mathrm{tr}(\mathbf{C})$ can be approximated by minimizing $b(\mathcal{A})$. However, there are local fluctuations of $\mathrm{tr}(\mathbf{C})$. Because of the fluctuations, the anchors selected by minimizing $b(\mathcal{A})$ may not be the ones minimizing $\mathrm{tr}(\mathbf{C})$, as seen in Fig. 1c and d. Therefore, the performance of the proposed approximation should be investigated.

3.1 Isotropic Discriminability

What is $b(\mathcal{A})$? By using relative-transformation decomposition, the location vector $\mathbf{s}$ can be reparameterized as

$$\mathbf{s}=\mathbf{U}\boldsymbol{\eta}+\mathbf{V}\boldsymbol{\zeta} \tag{9}$$

where $\boldsymbol{\eta}\in\mathbb{R}^{2n-3}$ and $\boldsymbol{\zeta}\in\mathbb{R}^3$ refer to the coordinates in the relative and transformation subspace, respectively.

Under the assumption that the deformation of the relative configuration is isotropically discriminable, *i.e.*, the FIM $\mathbf{J}_{\boldsymbol{\eta}}=\alpha\mathbf{I}_{2n-3},\ \alpha>0$, and no information on the global transformation is available, *i.e.*, the FIM $\mathbf{J}_{\boldsymbol{\zeta}}=\mathbf{0}$, we have

$$\mathbf{J}_{\mathbf{s}}=\alpha\mathbf{U}\mathbf{U}^T. \tag{10}$$

Throughout this paper, we ignore the factor α without loss of generality.

After setting m anchors, we get the CRLB of $\mathbf{s}$ from (6), whose trace is just $b(\mathcal{A})$. Comparing (5) and (10), we find that the approximation $b(\mathcal{A})$ is equivalent to an isotropic discriminability approximation of the deformation of the relative configuration, where the similarity can be evaluated by the eigenvalue ratio λ_1/λ_{2n-3}.

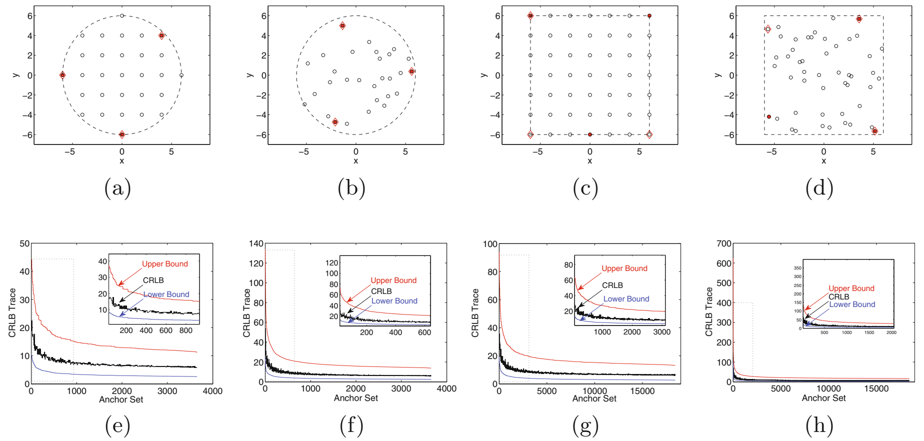

Fig. 1. Four examples: Fig (a), (b), (c), and (d) present the node configurations, where the anchor triplet selected by minimizing $b(\mathcal{A})$ (red empty diamonds: $\diamond$) is compared with the one obtained by minimizing $\mathrm{tr}(\mathbf{C})$ (red solid circles: $\bullet$). Figure (e), (f), (g), and (h) provide $\mathrm{tr}(\mathbf{C})$, its lower bound $\lambda_1^{-1} b(\mathcal{A})$, and upper bound $\lambda_{2n-3}^{-1} b(\mathcal{A})$ as the functions of all anchor triplets selected from the nodes, sorted by the descending order of $b(\mathcal{A})$. (Color figure online)

3.2 Performance Analysis

The performance of the approximation (8) can be quantified through the CRLB ratio $\frac{\mathrm{tr}(\mathbf{C}(\mathcal{A}_b))}{\mathrm{tr}(\mathbf{C}(\mathcal{A}_c))}$, where the numerator is the trace of the CRLB (6) corresponding to the anchor set $\mathcal{A}_b$ obtained by minimizing $b(\mathcal{A})$ and the denominator referring to the anchor set $\mathcal{A}_c$ obtained by minimizing the CRLB trace directly. This performance metric is bounded as below.

Proposition 2. *The CRLB ratio is bounded as*

$$1 \leq \frac{\mathrm{tr}(\mathbf{C}(\mathcal{A}_b))}{\mathrm{tr}(\mathbf{C}(\mathcal{A}_c))} \leq \frac{\lambda_1}{\lambda_{2n-3}}. \tag{11}$$

The proof is given in Appendix B.

The eigenvalue ratio λ_1/λ_{2n-3} is independent of the anchor selection. When λ_1/λ_{2n-3} approaches 1, the anchor set selected by minimizing $b(\mathcal{A})$ would be close to the optimal one. But in practice, although the CRLB ratios of the selected anchors are 1, 1, 1.0033, and 1.0287, the corresponding upper bounds λ_1/λ_{2n-3} are 4.3949, 5.4152, 4.9110, and 6.0145, respectively in Fig. 1a, b, c and d. Compared with the CRLB ratio, it seems that the upper bound λ_1/λ_{2n-3} tends to be conservative.

In fact, there is a negative result.

Proposition 3. *For fully connected networks, the eigenvalue ratio λ_1/λ_{2n-3} is bounded as*

$$\lambda_1/\lambda_{2n-3} \geq 2. \tag{12}$$

The proof can be found in Appendix C.

The equality in (12) holds under the condition that the nodes are uniformly deployed on a circle. As seen in Fig. 2, 49 nodes are uniformly deployed on a circle, with all pairwise distance measurements available. In this case, $\lambda_1/\lambda_{2n-3} = 2$, where $\lambda_1 = 49$ and $\lambda_{2n-3} = 24.5$. From Fig. 2b, it can be seen that the upper bound $\lambda_{2n-3}^{-1} b(\mathcal{A})$ is close to the CRLB trace $\mathrm{tr}(\mathbf{C})$, thus the anchor set selected by minimizing $b(\mathcal{A})$ is the optimal in this trivial case.

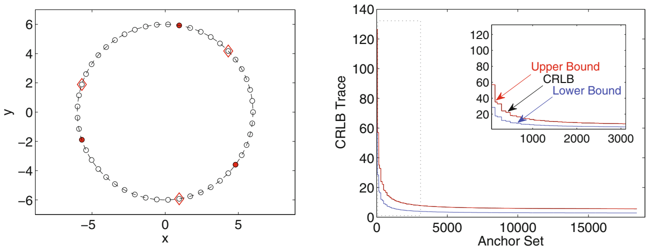

(a) (b)

Fig. 2. Special case: Fig (a) presents the configuration of 49 nodes uniformly deployed on a ring, where the anchor triplet selected by minimizing $b(\mathcal{A})$ (red empty diamonds: ◇) equals to (up to a symmetry) the one obtained by minimizing $\mathrm{tr}(\mathbf{C})$ (red solid circles: ●). Figure (b) provides $\mathrm{tr}(\mathbf{C})$, its lower bound $\lambda_1^{-1} b(\mathcal{A})$, and upper bound $\lambda_{2n-3}^{-1} b(\mathcal{A})$ as the functions of all anchor triplets selected from the nodes, sorted by the descending order of $b(\mathcal{A})$. (Color figure online)

4 Conclusion

In this paper, a uniform perimeter anchor deployment strategy is proved to be the optimal to fixing an isotropically discriminable relative configuration with randomly deployed nodes onto a two-dimensional plane. This strategy is used for anchor selection in cooperative location, where there exists deviation coming from the fact that the relative configuration specified by the internode distances is not isotropically discriminable in general. Theoretical analysis is performed to investigate the deviation, and more work is still needed to investigate the performance of the uniform perimeter anchor deployment strategy in future.

Acknowledgment. This research is partially supported by National Natural Science Foundation of China under Grant No. 61300170 and No. 61501005, Educational Commission of Anhui Province of China under Grant TSKJ2015B10, University Provincial Natural Science Foundation of Anhui Province under Grant No. KJ2016A057, and Research Starting Foundation of Anhui Polytechnic University under Grant No. 2015YQQ010.

A Derivation of (7) and (8)

From (5), we have

$$\lambda_{2n-3}\mathbf{U}\mathbf{U}^T \le \mathbf{J_s} \le \lambda_1 \mathbf{U}\mathbf{U}^T \tag{13}$$

and thus

$$\lambda_{2n-3}\mathbf{H}^T\mathbf{U}\mathbf{U}^T\mathbf{H} \le \mathbf{H}^T\mathbf{J_s}\mathbf{H} \le \lambda_1 \mathbf{H}^T\mathbf{U}\mathbf{U}^T\mathbf{H}. \tag{14}$$

Note that $\mathbf{C} = \left(\mathbf{H}^T\mathbf{J_s}\mathbf{H}\right)^{-1}$, we get

$$\lambda_1^{-1} \le \frac{\mathrm{tr}\left(\mathbf{C}\right)}{b(\mathcal{A})} \le \lambda_{2n-3}^{-1} \tag{15}$$

after performing inversion and trace operation of (14).

To derive an analytical representation of $b(\mathcal{A})$, we use an column orthonormalized version of $\mathbf{V}$

$$\mathbf{V} = \left[\frac{1}{\sqrt{n}}\mathbf{1}_x, \frac{1}{\sqrt{n}}\mathbf{1}_y, \frac{\mathbf{v_s} - \frac{1}{n}\mathbf{1}_x^T\mathbf{v_s}\mathbf{1}_x - \frac{1}{n}\mathbf{1}_y^T\mathbf{v_s}\mathbf{1}_y}{\|\mathbf{v_s} - \frac{1}{n}\mathbf{1}_x^T\mathbf{v_s}\mathbf{1}_x - \frac{1}{n}\mathbf{1}_y^T\mathbf{v_s}\mathbf{1}_y\|}\right] \tag{16}$$

and thus $\mathbf{H}^T\mathbf{U}\mathbf{U}^T\mathbf{H} = \mathbf{I}_{2(n-m)} - \mathbf{H}^T\mathbf{V}\mathbf{V}^T\mathbf{H}$.

By applying the block matrix inversion formula and some matrix manipulations, we get

$$\mathrm{tr}\left(\left(\mathbf{I}_{2(n-m)} - \mathbf{H}^T\mathbf{V}\mathbf{V}^T\mathbf{H}\right)^{-1}\right) = \mathrm{tr}\left(\left(\mathbf{V}^T\left(\mathbf{I}_{2n} - \mathbf{H}\mathbf{H}^T\right)\mathbf{V}\right)^{-1}\right) + 2(n-m) - 3. \tag{17}$$

Note that

$$\mathbf{V}^T\left(\mathbf{I}_{2n} - \mathbf{H}\mathbf{H}^T\right)\mathbf{V} = \frac{m}{n}\begin{bmatrix} 1 & 0 & -\frac{\bar{s}_{\mathcal{A},y}-\bar{s}_y}{\rho} \\ 0 & 1 & \frac{\bar{s}_{\mathcal{A},x}-\bar{s}_x}{\rho} \\ -\frac{\bar{s}_{\mathcal{A},y}-\bar{s}_y}{\rho} & \frac{\bar{s}_{\mathcal{A},x}-\bar{s}_x}{\rho} & \frac{\tilde{\rho}_{\mathcal{A}}^2}{\rho^2} \end{bmatrix} \tag{18}$$

where $\bar{s}_x = \frac{1}{n}\sum_{i=1}^n s_{i,x}$, $\bar{s}_y = \frac{1}{n}\sum_{i=1}^n s_{i,y}$, $\bar{s}_{\mathcal{A},x} = \frac{1}{m}\sum_{j\in\mathcal{A}} s_{j,x}$, $\bar{s}_{\mathcal{A},y} = \frac{1}{m}\sum_{j\in\mathcal{A}} s_{j,y}$, $\rho^2 = \frac{1}{n}\sum_{i=1}^n (s_{i,x}-\bar{s}_x)^2 + (s_{i,y}-\bar{s}_y)^2$, and $\tilde{\rho}_{\mathcal{A}}^2 = \frac{1}{m}\sum_{j\in\mathcal{A}}(s_{j,x} - \bar{s}_x)^2 + (s_{j,y}-\bar{s}_y)^2$, we get

$$\left(\mathbf{V}^T\left(\mathbf{I}_{2n} - \mathbf{H}\mathbf{H}^T\right)\mathbf{V}\right)^{-1} = \frac{n}{m}\begin{bmatrix} 1 + \frac{\left(\bar{s}_{\mathcal{A},y}-\bar{s}_y\right)^2}{\rho_{\mathcal{A}}^2} & \frac{n(\bar{s}_{\mathcal{A},x}-\bar{s}_x)(\bar{s}_{\mathcal{A},y}-\bar{s}_y)}{-\rho_{\mathcal{A}}^2} & \frac{\rho(\bar{s}_{\mathcal{A},y}-\bar{s}_y)}{\rho_{\mathcal{A}}^2} \\ \frac{n(\bar{s}_{\mathcal{A},x}-\bar{s}_x)(\bar{s}_{\mathcal{A},y}-\bar{s}_y)}{-\rho_{\mathcal{A}}^2} & 1 + \frac{\left(\bar{s}_{\mathcal{A},x}-\bar{s}_x\right)^2}{\rho_{\mathcal{A}}^2} & \frac{\rho(\bar{s}_{\mathcal{A},x}-\bar{s}_x)}{-\rho_{\mathcal{A}}^2} \\ \frac{\rho(\bar{s}_{\mathcal{A},y}-\bar{s}_y)}{\rho_{\mathcal{A}}^2} & \frac{\rho(\bar{s}_{\mathcal{A},x}-\bar{s}_x)}{-\rho_{\mathcal{A}}^2} & \frac{\rho^2}{\rho_{\mathcal{A}}^2} \end{bmatrix} \tag{19}$$

where

$$\rho_{\mathcal{A}}^2 = \frac{1}{m}\sum_{j\in\mathcal{A}}(s_{j,x} - \bar{s}_{\mathcal{A},x})^2 + (s_{j,y} - \bar{s}_{\mathcal{A},y})^2. \tag{20}$$

Substituting (19) into (17), we get (8).

B Proof of (11)

Let $\mathcal{A}_c$ and $\mathcal{A}_b$ denote the anchor set obtained by minimizing $\mathrm{tr}(\mathbf{C})$ and $b(\mathcal{A})$, respectively. After replacing $\mathbf{C}$ with $\mathbf{C}(\mathcal{A})$ to stress its dependence on the anchor selection, we get

$$\frac{\mathrm{tr}(\mathbf{C}(\mathcal{A}_b))}{\mathrm{tr}(\mathbf{C}(\mathcal{A}_c))} \geq 1 \tag{21}$$

$$\frac{b(\mathcal{A}_b)}{b(\mathcal{A}_c)} \leq 1. \tag{22}$$

From (7), we have

$$\mathrm{tr}(\mathbf{C}(\mathcal{A}_c)) \geq \lambda_1^{-1} b(\mathcal{A}_c) \tag{23}$$

$$\mathrm{tr}(\mathbf{C}(\mathcal{A}_b)) \leq \lambda_{2n-3}^{-1} b(\mathcal{A}_b) \tag{24}$$

and thus

$$\frac{\mathrm{tr}(\mathbf{C}(\mathcal{A}_b))}{\mathrm{tr}(\mathbf{C}(\mathcal{A}_c))} \leq \frac{\lambda_{2n-3}^{-1} b(\mathcal{A}_b)}{\lambda_1^{-1} b(\mathcal{A}_c)} \leq \frac{\lambda_1}{\lambda_{2n-3}} \tag{25}$$

where the right inequality is obtained by using (22).

From (21) and (25), we get

$$1 \leq \frac{\mathrm{tr}(\mathbf{C}(\mathcal{A}_b))}{\mathrm{tr}(\mathbf{C}(\mathcal{A}_c))} \leq \frac{\lambda_1}{\lambda_{2n-3}}. \tag{26}$$

C Proof of (12)

Without loss of generality, we set $\sigma^2 = 1$. Then for a fully connected network, it can be verified that n is an eigenvalue of $\mathbf{J_s}$ with eigenvector proportional to $\mathbf{s} - \frac{1}{n}\mathbf{1}_x\mathbf{1}_x^T\mathbf{s} - \frac{1}{n}\mathbf{1}_y\mathbf{1}_y^T\mathbf{s}$. Note that the ith 2-by-2 diagonal block of $\mathbf{J_s}$ can be rewritten as $\sum_{j,j\neq i} \boldsymbol{\tau}_{i,j}\boldsymbol{\tau}_{i,j}^T$, and

$$\mathrm{tr}(\boldsymbol{\tau}_{i,j}\boldsymbol{\tau}_{i,j}^T) = \mathrm{tr}(\boldsymbol{\tau}_{i,j}^T\boldsymbol{\tau}_{i,j}) = 1, i \neq j \tag{27}$$

we have

$$\mathrm{tr}(\mathbf{J_s}) = \sum_{i=1}^{n} \mathrm{tr}(\sum_{j,j\neq i} \boldsymbol{\tau}_{i,j}\boldsymbol{\tau}_{i,j}^T) = n(n-1). \tag{28}$$

Since $\mathbf{J_s}$ is positive semidefinite with eigenvalues $\lambda_1 \geq \lambda_2 \geq \cdots \geq \lambda_{2n-3} \geq \lambda_{2n-2} = \lambda_{2n-1} = \lambda_{2n} = 0$, we get

$$\lambda_{2n-3} = \min_{i=2,3,\ldots,2n-3} \lambda_i \leq \frac{n(n-1)-n}{2n-4} = \frac{n}{2}. \tag{29}$$

Therefore, $\lambda_1/\lambda_{2n-3} \geq 2$ because $\lambda_1 \geq n$.

References

1. Patwari, N., Ash, J.N., Kyperountas, S., Hero III, A.O., Moses, R.L., Correal, N.S.: Locating the nodes: cooperative localization in wireless sensor networks. IEEE Signal Process. Mag. **22**(4), 54–69 (2005)
2. Patwari, N., Hero III, A.O., Perkins, M., Correal, N.S., O'Dea, R.J.: Relative location estimation in wireless sensor networks. IEEE Trans. Signal Process. **51**(8), 2137–2148 (2003)
3. Zhang, P., Wang, Q.: On using the relative configuration to explore cooperative localization. IEEE Trans. Signal Process. **62**(4), 968–980 (2014)
4. Ash, J.N., Moses, R.L.: On the relative and absolute positioning errors in self-localization systems. IEEE Trans. Signal Process. **56**(11), 5668–5679 (2008)
5. Jackson, B., Jordán, T.: Graph theoretic techniques in the analysis of uniquely localizable sensor networks. In: Mao, G., Fidan, B. (eds.) Localization Algorithms and Strategies for Wireless Sensor Networks, pp. 146–173. IGI Global (2009)
6. Eren, T., Goldenberg, O.K., Whiteley, W., Yang, Y.R., Morse, A.S., Anderson, B.D.O., Belhumeur, P.N.: Rigidity, computation, and randomization in network localization. In: Proceedings of IEEE Conference on Computer Communication, vol. 4, pp. 2673–2684 (2004)
7. Yang, Z., Liu, Y., Li, X.Y.: Beyond trilateration: on the localizability of wireless ad hoc networks. IEEE/ACM Trans. Netw. **18**(6), 1806–1814 (2010)
8. Aspnes, J., Eren, T., Goldenberg, D., Morse, A., Whiteley, W., Yang, Y., Anderson, B.D.O., Belhumeur, P.: A theory of network localization. IEEE Trans. Mobile Comput. **5**(12), 1663–1678 (2006)
9. Huang, M., Chen, S., Wang, Y.: Minimum cost localization problem in wireless sensor networks. Ad Hoc Netw. **9**(3), 387–399 (2011)
10. Yang, Z., Liu, Y.: Understanding node localizability of wireless ad hoc and sensor networks. IEEE Trans. Mobile Comput. **11**(8), 1249–1260 (2012)
11. Savvides, A., Garber, W., Adlakha, S., Moses, R., Srivastava, M.B.: On the error characteristics of multihop node localization in ad-hoc sensor networks. In: Zhao, F., Guibas, L. (eds.) IPSN 2003. LNCS, vol. 2634, pp. 317–332. Springer, Heidelberg (2003). doi:10.1007/3-540-36978-3_21
12. Li, X.L., Shi, H.C., Shang, Y.: Selective anchor placement algorithm for ad-hoc wireless sensor networks. In: Proceedings of IEEE International Confernce on Communications, pp. 2359–2363 (2008)
13. Chan, F., So, H.C., Ma, W.K.: A novel subspace approach for cooperative localization in wireless sensor networks using range measurements. IEEE Trans. Signal Process. **57**(1), 260–269 (2009)
14. Zhang, P., Lu, J., Wang, Q.: Performance bounds for relative configuration and global transformation in cooperative localization. ICT Express **2**(1), 14–18 (2016). special Issue on Positioning Techniques and Applications
15. Ash, J.N., Moses, R.L.: On optimal anchor node placement in sensor localization by optimization of subspace principal angles. In: Proceedings of IEEE International Conference on Acoustics of Speech, Signal Processing, pp. 2289–2292 (2008)
16. Zhang, P., Wang, Q.: Anchor selection with anchor location uncertainty in wireless sensor network localization. In: Proceedings of IEEE International Conference on Acoustics, Speech, Signal Processing, pp. 4172–4175 (2011)